Chapter 5

Bubble Dynamics in a Narrow Rectangular Channel

Xu Jianjun, Xie Tianzhou, Chen Bingde and Bao Wei

Additional information is available at the end of the chapter

http://dx.doi.org/10.5772/intechopen.74608

Abstract

It is very important to study the bubble dynamics in order to understand the physical process of boiling heat transfer in a narrow channel. Experimental and theoretical studies on bubble dynamics in a narrow rectangular channel are proposed. The cross section of the narrow rectangular channel is 2 mm × 8 mm. A high speed digital camera is applied to capture bubble behaviors from the narrow side and wide side of the narrow rectangular channel. Bubble growth rate, bubble departure diameter, bubble interface parameter and others are obtained according to the observation. A force balance analysis on a growing bubble is proposed to predict the bubble departure diameter and sliding bubble velocity, and the predicted results agree with the experimental data. Thus, the mechanism of bubble departure, slide and lift-off behavior in a narrow rectangular channel can be explained by the analysis of forces.

Keywords: narrow channel, bubble dynamics, force balance

1. Introduction

Thermal hydraulics and safety analysis are important in nuclear reactor design and operation. There have been active investigations on nuclear thermal hydraulics and safety analysis in different core fuel elements. The rod bundles with grid spacers and plate-type fuel elements are frequently encountered at the aspect of developing new type nuclear reactor. The coolant channels of the plate-type fuel element are composed of some typical narrow rectangular channels, and the flow and heat transfer in a narrow rectangular channel is also widely employed in the compact evaporators and heat exchangers. So it is important to perform the thermal hydraulic study of boiling heat transfer in the narrow rectangular channels.

During the last decades, there were a lot of investigations focusing on two-phase flow and boiling heat transfer in narrow rectangular channels in published literatures [1–14]. The results

show that two-phase flow and boiling heat transfer in a narrow channel is a very complex physical process. Some researchers think that boiling heat transfer in a narrow channel are different from that in an ordinary sized channel and the boiling heat transfer mechanism in a narrow rectangular channel is not fully understood.

In order to understand the physical process of boiling heat transfer in a narrow channel, and it is important to study the bubble growth, departure and lift-off behavior by using the visualized technology. Over the last half century, a lot of studies of bubble dynamics have been conducted, and this kind of study is significant to understand the boiling heat transfer mechanism. It is the fundamental for understanding and predicting the boiling heat transfer correctly. However, most of these studies have been focused on observation of bubble behaviors in an ordinary sized channel. In our previous work, bubble characteristics in narrow rectangular channel were visually studied, and the results showed that the bubbles departing from the nucleation sites always slid along the heating wall [15]. Some researchers presented the importance of the sliding bubble to enhance heat transfer in nucleate boiling [16–20], the results showed that turbulence caused by sliding bubbles could be an important mechanism in enhancing heat transfer. The effect of sliding bubbles on boiling heat transfer in a narrow channel will be more important than that in an ordinary sized channel because of the smaller cross section size.

It is known that the analysis of forces acting on a single bubble is a promising approach to sufficiently understand the mechanism of bubble motion. Levy [21] first proposed a model for the prediction of bubble departure diameter based on the balance of forces, including the buoyancy, surface tension force and drag force. Klausner et al. [22] built the models of force balance to predict the bubble departure diameter and lift-off diameter, and there have been active investigations on the analysis of forces balance [14, 23–25], and these researches implies that bubble interface parameters were required as the input parameters in order to solve this model, including the bubble inclination angle, upstream contact angle, downstream contact angle and bubble contact diameter. It is also important to develop the wall heat flux partitioning model and the interfacial area transport equation for using computational fluid dynamics (CFD) code.

These studies in the above literatures have not provided an adequately detailed understanding of boiling heat transfer in a narrow rectangular channel. The present study showed bubble growth, departure, sliding and lift-off behaviors in a narrow rectangular channel, and the mechanism of bubble departure and lift-off from the heating wall was discussed based on the analysis of forces acting on the bubble.

2. Experimental facilities and measuring system

Figure 1 shows a schematic of the test section of the narrow rectangular channel. The cross section of the narrow rectangular channel was 2×8 mm^2, which was fabricated in an optical quartz glass. Both the wide side and the gap side of the optical quartz glass were polished to improve the transparency. Bubble behavior was visually observed from the wide side and gap

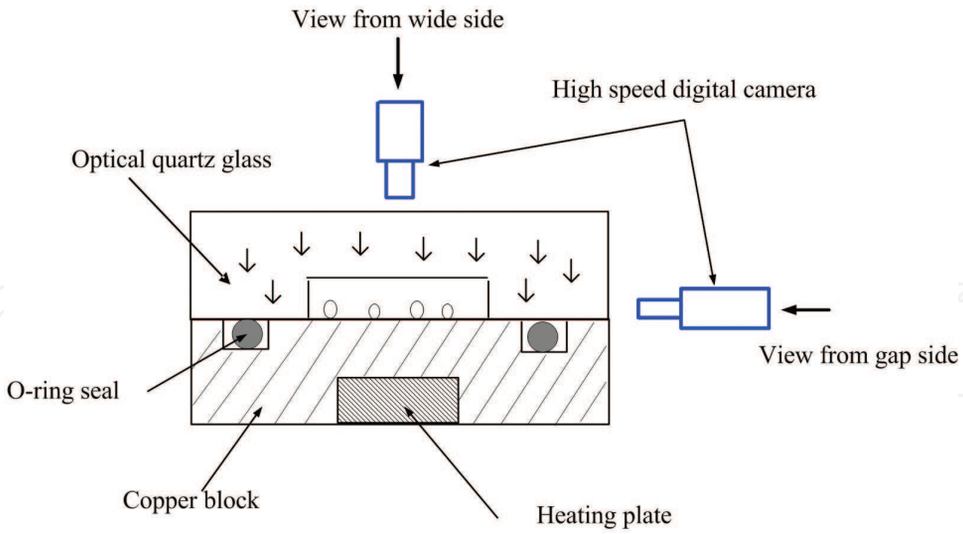

Figure 1. Schematic diagram of test section.

side of the rectangular channel. The observation windows were made of optical quartz glass. The width of the narrow rectangular channel is 8 mm and height is 2 mm. The same experimental apparatus was described to investigate the bubble dynamics in the previous study of the authors [13].

In the present work, the experiment pressure was atmospheric pressure. The range of the liquid subcooling of the inlet of the test section was 10–40°C. The range of mass flux was 129–706 kg/m^2 s. Temperatures at the wall, inlet, and outlet of the test section were registered by 1 mm diameter T-type thermocouples, which were calibrated and a uncertainty of 0.5°C for all thermocouples. The uncertainty in the heat supplied to the test section was less than ±0.9%. The heat loss of the test section was estimated to within 7% of the total of the heating power in the present study. Flow rate was measured by a venturimeter and the uncertainty was less than

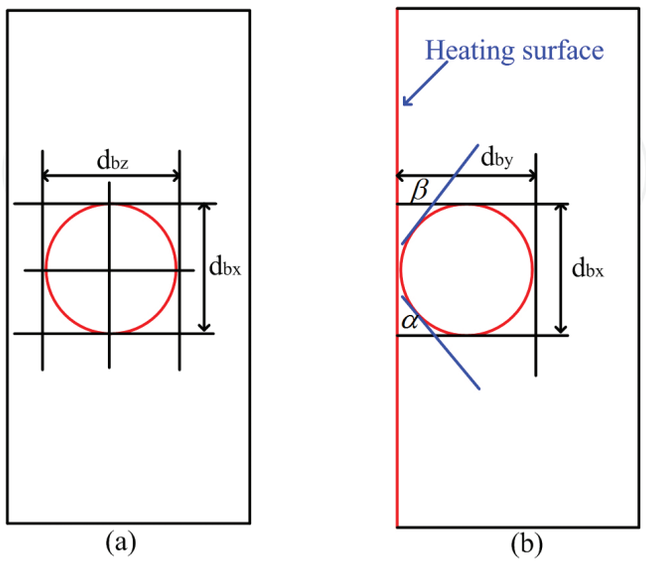

Figure 2. Definition of bubble equivalent diameter.

±0.8% of the full scale range. The pressure of test section was measured by a pressure transmitter, and the uncertainty was less than ±0.5 kPa of the full scale range.

A high speed digital camera (Micro-NIKKOR lens 200 mm 1:1) was used to capture bubble dynamics. The successive typical bubble images were obtained by using a high speed digital camera. The bubble dynamics can be obtained from the wide side and gap side of the narrow rectangular channel, respectively. A picture of the vernier caliper was captured with the high speed digital camera, and the scale factor was defined by the image of vernier caliper. The real dimension of bubble was obtained with the scale factor. The bubble dynamics was captured with a speed of 3800 fps (frames per second). The 576 × 576 pixel picture corresponds to a 7.2 mm × 7.2 mm recorded field in real dimension. **Figure 2** defined the bubble equivalent diameter as following:

$$\frac{\pi}{6}d^3 = \frac{\pi}{6}d_{bx}d_{bz}^2 \Rightarrow d = \sqrt[3]{d_{bx}d_{bz}^2} \quad (if \quad d_{bx} > d_{bz}) \tag{1}$$

$$\frac{\pi}{6}d^3 = \frac{\pi}{6}d_{bx}d_{by}^2 \Rightarrow d = \sqrt[3]{d_{bx}d_{by}^2} \quad \left(if \quad d_{bx} > d_{by}\right) \tag{2}$$

The ratio R of the bubble contact diameter to the bubble departure diameter is expressed as:

$$R = d_w/d_0 \tag{3}$$

3. Experimental observation of bubble dynamics

3.1. Bubble growth and departure

A series of images of a typical bubble growing at the nucleation site is obtained by observation from the narrow side of the rectangular channel, as shown in **Figure 3**. The bubble shape is almost spherical when the bubble is growing at the nucleation sites. The contact diameter between the bubble base and heating wall is observed when the bubble is growing at the nucleation site. The interface parameters of typical bubbles just departing from the nucleation

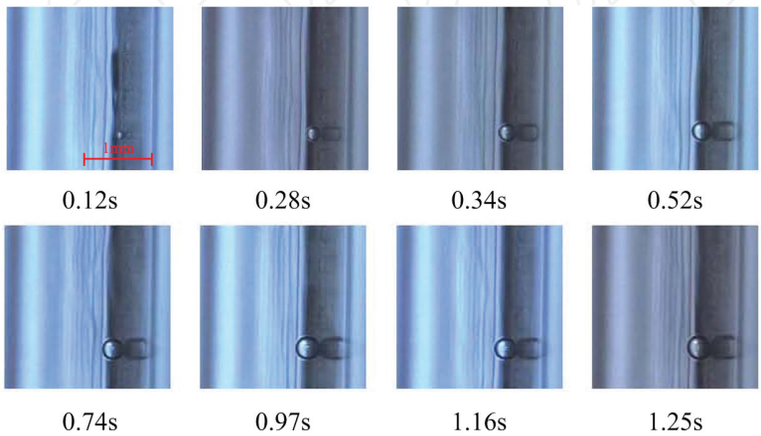

Figure 3. Visualization of bubble growth and departure from narrow side.

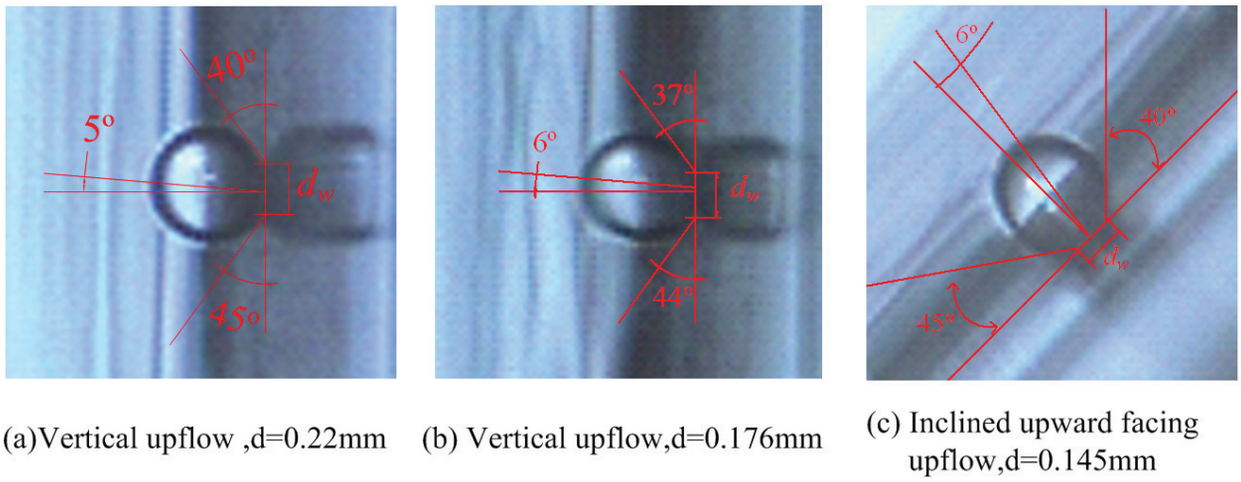

Figure 4. Bubble contact angle and inclination angle [14].

site, such as the bubble inclination angle, upstream contact angle, downstream contact angle, and bubble contact diameter, are measured by observation [14], as shown in **Figure 4**. The bubble upstream contact angle varies from 44° to 45°, the bubble downstream contact angle varies from 37° to 40°, the inclination angle varies from 5° to 6°, the range of R in the current experiment is about 0.41–0.5, and the average of R is about 0.45.

Figure 5 shows the effect of heat flux on bubble growth at the same nucleation site [14]. The bubble growth rate increases with increasing heat flux. The bubble departure time decreases with increasing heat flux, and so the bubble departure diameter decreases with increasing heat flux. According to Zuber's model [26], the bubble growth rates can be approximated by a power law curve fit, and the range of the power law varies from about 0.34 to 0.684.

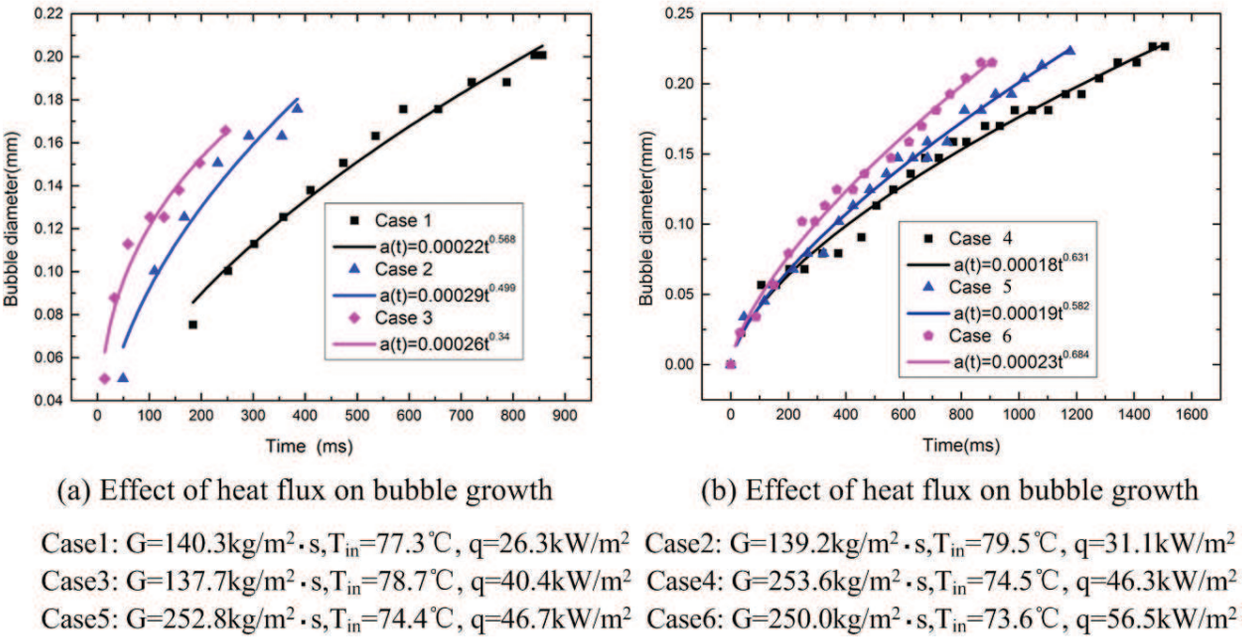

Figure 5. Bubble growth diameter with time [14].

3.2. Sliding bubble behavior in vertical channel

The images of typical sliding bubbles motion at the same observation window are obtained from the narrow side of the rectangular channel, as shown in **Figure 6**. After a bubble departs from the nucleation site, it always slides along the heating wall. The typical bubble sliding phenomenon in vertical upflow boiling is observed at low heat flux in the isolated bubble region [13]. During the bubble sliding along the heating wall, the bubble contact diameter between the bubble base and heating wall is observed. The sliding bubble diameter increases with increasing heat flux. The number of sliding bubbles increases gradually with increasing heat flux. The sliding bubbles start to coalescence, and sliding bubbles become the larger after coalescence, kenning et al. [19] considered it as the main model for influence of the thermal boundary layer reformation near the wall due to sliding bubble motion. The phenomenon of bubble lift-off from the heating wall is not observed, which shows the effect of the sliding bubble interaction among the sliding bubbles is also little in the isolated bubble region with low heat flux. It is known that the turbulent effect is strong with increasing number of bubbles for the high heat flux, which maybe results in bubble lift-off from the heating wall.

The shape of the small sliding bubble appears spherical, but it is elongated in the direction normal to the heating wall with increasing bubble diameter. When the bubble slides along the heating wall, the upstream contact angle and downstream contact angle of the sliding bubble is almost equal, and so the inclination angle of the sliding bubble approaches to zero. In the present work, the confined bubble growing and sliding motion in the narrow rectangular channel is not observed.

Figure 7 shows the sliding bubble velocity under different bubble diameter with time, as is seen from **Figure 7**, the sliding bubble velocity increase obviously at the initial moment, but the

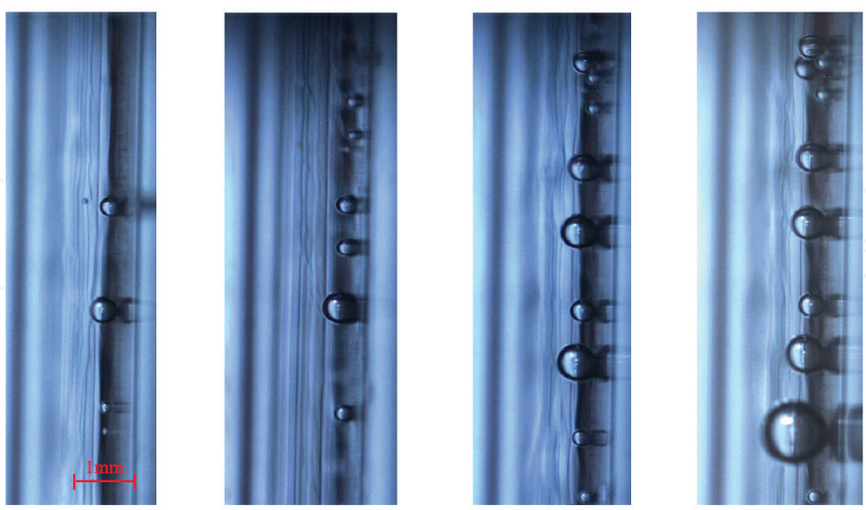

Figure 6. Typical sliding bubble with increasing heat flux.

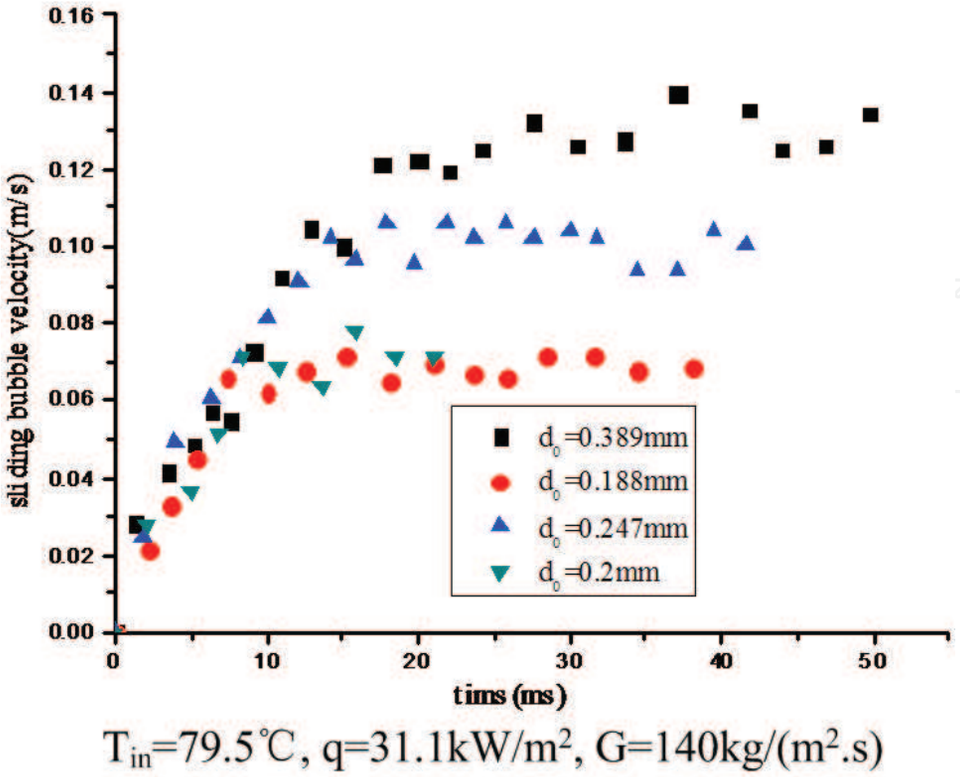

Figure 7. Sliding bubble velocity with time.

sliding bubble velocity approach asymptote, ultimately. The influence of the sliding bubble diameter on the velocity is larger. The sliding bubble ultimate velocity increase with increasing bubble diameter, which shows the importance of buoyancy in the flow direction. The velocity of sliding bubble (d_0 = 0.389 mm) approaches to the bulk liquid velocity.

3.3. Bubble lift-off behavior

In inclined 45° upward facing upflow boiling, the phenomenon on bubble lift-off from the heating wall is observed from the narrow side of the rectangular channel at the same observation window, as is shown in **Figure 8**. After a bubble slides some distance, it tends to lift-off from the heating wall, and the buoyancy at the direction normal to the surface is responsible for the bubble lift-off in inclined 45° upward facing heating wall. The bubble velocity will increase when the bubble lifts off from the heating wall. The condensation phenomenon on the interface of the lift-off bubble occurs when the bulk flow is subcooled, which results in the change of bubble shape.

In vertical downflow boiling, the images of bubbles are obtained from the same observation window with the different heat flux, as is shown in **Figure 9**. After a bubble departs from the nucleation site, it tends to lift-off from the surface. When the bubble lifts off from the heating wall, the shadow of the bubble is observed on the heating wall. The bubble size is small due to the condensation on the interface of the lift-off bubble. The bubble velocity in vertical downflow boiling is small due to the opposite direction of the buoyancy and drag forces acting on the

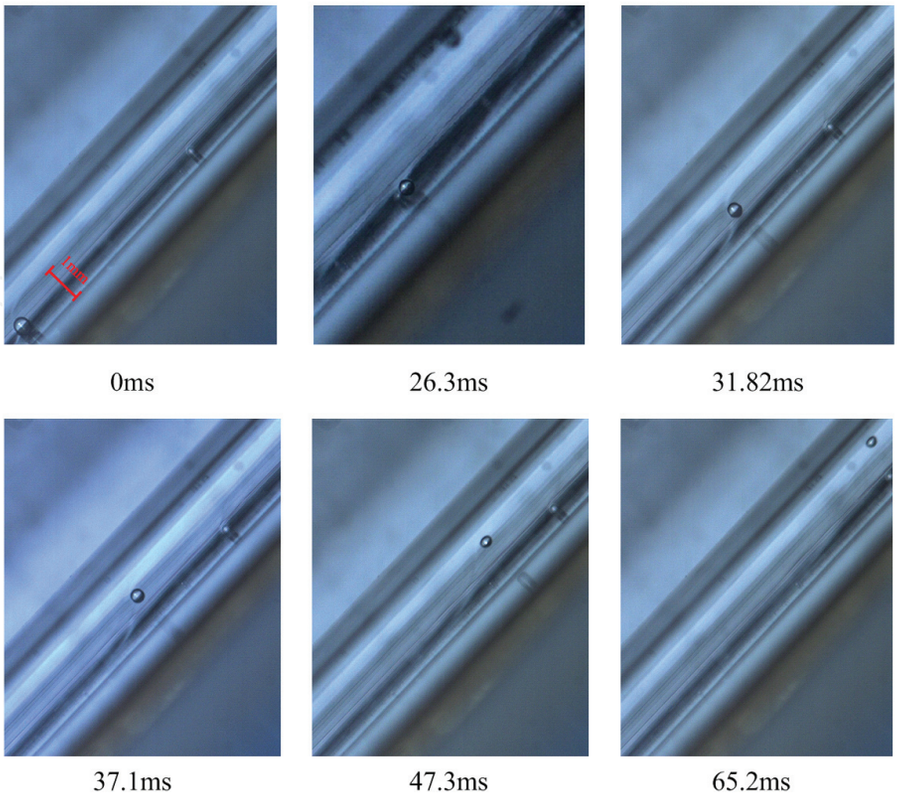

Figure 8. Single bubble motion in inclined 45° upward facing upflow boiling.

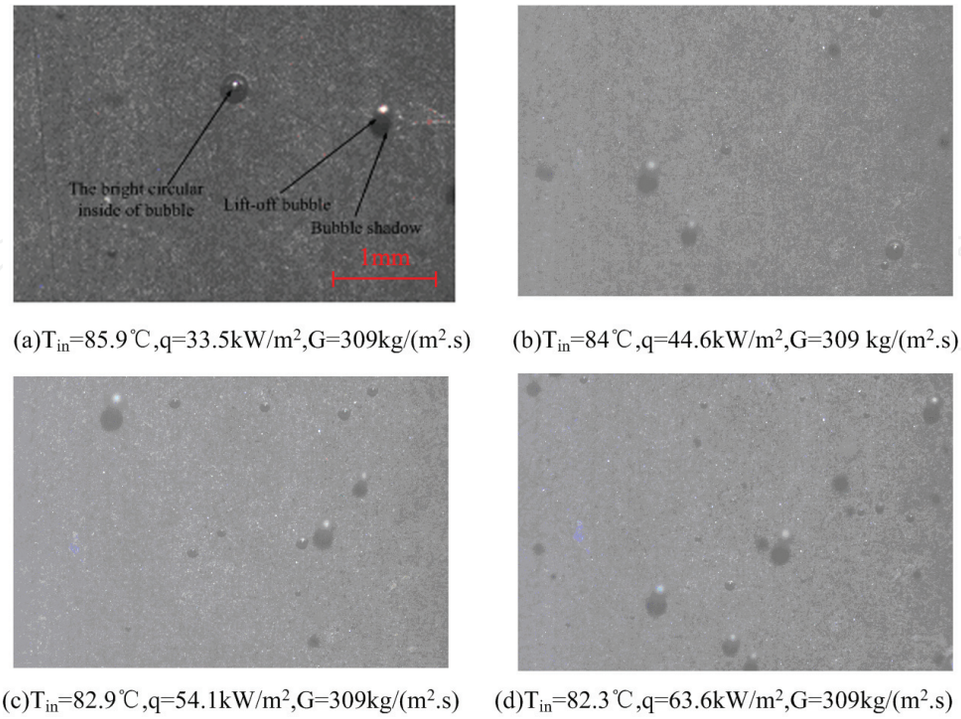

Figure 9. Bubble motion in vertical downflow boiling.

bubble. The local fluid velocity is always higher than that of the bubble velocity, and so the shear lift force is the driving force to promote bubble lift-off from the heating wall.

4. Analysis of force acting on the bubble

4.1. Balance of forces acting on a single bubble

The forces acting on a single bubble are schematically shown in **Figure 10**. Different forces acting on a bubble in the directions parallel and normal to a heating wall are analyzed, and the force in the x and y directions are evaluated as following:

$$\sum F_x = F_{bx} + F_{sx} + F_{amx} + F_{qs} = m_b \frac{dv_x}{dt} \tag{4}$$

$$\sum F_y = F_{bx} + F_{sy} + F_{amy} + F_{sl} + F_h + F_{cp} = m_b \frac{dv_y}{dt} \tag{5}$$

where F_b is the buoyancy force, F_s is the surface tension force, F_{am} is the added-mass force, F_{qs} is the quasi-steady drag force, m_b is the mass of the sliding bubble, v_x is the velocity of displacement of the center of mass of the bubble in the x direction, t is the time, F_{sl} is the shear lift force, F_h is the force due to the hydrodynamic pressure, F_{cp} is the contact pressure force, θ is the incline angle of the bubble, α is the upstream contact angle, β is the downstream contact angle, v_y is the velocity of displacement of the center of mass of the bubble in the y direction, d_w is the contact diameter, $u(y)$ is the local liquid velocity profile near the wall, and Φ is the incline angle of the heating wall.

4.1.1. Buoyancy

The buoyancy acting on a bubble due to the surrounding liquid is expressed as

$$F_b = (\rho_l - \rho_v) V_b g \tag{6}$$

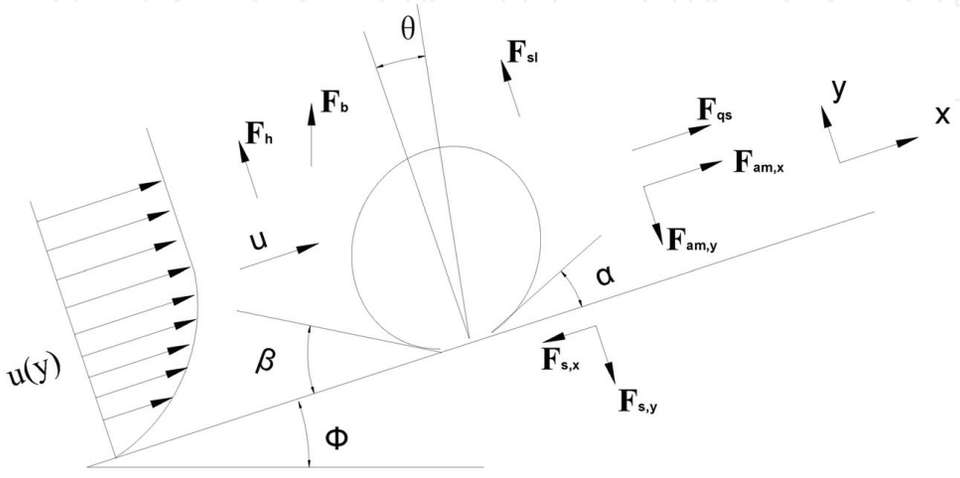

Figure 10. Force acting on a bubble.

where ρ_l is the density of liquid, ρ_v is the density of the vapor bubble, g is the gravitational acceleration, and V_b is the bubble volume.

4.1.2. Surface tension force

The surface tension forces at x and y directions are given as follows [22]:

$$F_{sx} = -d_w \sigma_{lv} \frac{\pi}{\alpha - \beta} \left(\cos\beta - \cos\alpha \right) \tag{7}$$

$$F_{sy} = -1.25 d_w \sigma_{lv} \frac{\pi(\alpha - \beta)}{\pi^2 - (\alpha - \beta)^2} \left(\sin\alpha + \sin\beta \right) \tag{8}$$

where σ_{lv} is surface tension.

4.1.3. Added-mass force

In order to estimate the added-mass force, Thorncroft and Klausner [23] developed the following expression by solving the inviscid flow problem for a growing sphere in a uniform, unsteady flow.

$$F_{am} = \frac{1}{2} \cdot \frac{4}{3} \pi \rho_l a^3 \left(\frac{dU}{dt} - \frac{dv_x}{dt} \right) + 2\pi \rho_l a^2 (U - v_x) \dot{a} \tag{9}$$

where the first term is the conventional added-mass force. The second term is the added-mass force due to bubble expansion. In the steady-state flow, dU/dt approaches zero. U is bulk liquid velocity, v_x is bubble velocity and a is the bubble growth radius.

When the bubble is growing at the nucleation site, the bubble's center of mass moves away from the heating wall and the added-mass force leads to the unsteady force in the direction normal to the wall. In keeping with convention, the added-mass force is referred to as the bubble growth force. Zeng et al. [27] suggested the growth force can be estimated from:

$$F_{am} = -\rho_l \pi a^2 \left(\frac{3}{2} C_S \dot{a}^2 + a\ddot{a} \right) \tag{10}$$

where $C_S = 20/3$.

4.1.4. Quasi-steady drag force

Delnoij et al. [28] suggested that the quasi-steady drag force can be estimated from:

$$F_{qs} = \frac{1}{2} C_D \rho_l \pi a^2 (u - v_x) |u - v_x| \tag{11}$$

$$C_D = \begin{cases} 240 & \mathrm{Re}_b \le 0.1 \\ \dfrac{24}{\mathrm{Re}_b} \left(1 + 0.15 \mathrm{Re}_b^{0.687} \right) & 0.1 < \mathrm{Re}_b \le 1000 \\ 0.44 & \mathrm{Re}_b > 1000 \end{cases} \tag{12}$$

$$\mathrm{Re}_b = \frac{2a(t)|u - v_x|}{\gamma} \tag{13}$$

where γ is the liquid kinematic viscosity, u is the velocity of local liquid, and Re_b is the bubble Reynolds number.

The local liquid velocity of the mass center of the bubble is estimated by using universal single-phase flow profile. The dimensionless velocity of different region is expressed by the following correlations:

$$u^+ = \begin{cases} y^+ & y^+ \le 5 \\ 5\ln y^+ - 3.05 & 5 < y^+ \le 30 \\ 2.5\ln y^+ + 5.5 & y^+ > 30 \end{cases} \tag{14}$$

$$u^+ = \frac{u}{u^*} = \frac{u}{\sqrt{\tau_w/\rho_l}} \tag{15}$$

$$y^+ = \frac{yu^*}{\gamma} = \frac{y\sqrt{\tau_w/\rho_l}}{\gamma} \tag{16}$$

$$u^* = \sqrt{\tau_w/\rho_l} \tag{17}$$

The wall shear stress can be calculated by the following expression

$$\tau_w = \frac{1}{2} C_f \rho_l U^2 \tag{18}$$

where C_f is the friction coefficient, which is calculated by the following expression

$$C_f = \lambda/4 \tag{19}$$

where λ is the friction factor. For a smooth surface, the friction factor is expressed by the following expression

$$\lambda = \begin{cases} 64/\mathrm{Re} & \mathrm{Re} < 2000 \\ 0.3163/\mathrm{Re}^{0.25} & 2000 \le \mathrm{Re} \le 100000 \end{cases} \tag{20}$$

$$\mathrm{Re} = \frac{UD_h}{\gamma} \tag{21}$$

where D_h *is* the hydraulic equivalent diameter.

4.1.5. Shear lift force

Saffman [29] developed an expression for the lift force on a particle in a low Reynolds number shear flow. Recently, Mei and Klausner [30] modified the Saffman model for a bubble as follows:

$$F_{sl} = \frac{1}{2} C_l \rho_l \pi a^2 (u - v_x)|u - v_x| \tag{22}$$

where C_l is the shear lift force coefficient and is defined as

$$C_l = 3.877 G_s^{1/2} \left(\mathrm{Re}_b^{-2} + 0.014 G_s^2 \right)^{1/4} \tag{23}$$

where

$$G_s = \left| \frac{du}{dy} \right| \frac{a(t)}{u - v_x} = \frac{1}{u - v_x} \frac{1}{k^+ u^+} \tag{24}$$

4.1.6. Contact pressure force

The contact pressure force due to the pressure difference inside and outside the bubble at the reference point over the contact area is given as follows [22]:

$$F_{cp} = \frac{\pi d_w^2}{4} \frac{2\sigma_{lv}}{r} \tag{25}$$

4.1.7. Hydrodynamic pressure force

Klausner et al. [22] suggested that the hydrodynamic force can be estimated from

$$F_h = \frac{1}{2} \frac{9}{4} \rho_l (u - v_x)|u - v_x| \frac{\pi d_w^2}{4} \tag{26}$$

The criteria of the bubble departing and sliding from the nucleation site was proposed by Klausner et al. [22]. The bubble remains attached to the nucleation site when the conditions $\sum F_x < 0$ and $\sum F_y < 0$. When the condition $\sum F_x = 0$ is violated prior to $\sum F_y = 0$, the bubbles will slide along the heating wall, and the criterion for bubble departure from the nucleation site is defined according to the condition $\sum F_x = 0$, at which point the bubble will departure from the nucleation site. When the condition $\sum F_y = 0$ is violated prior to $\sum F_x = 0$, the bubbles will lift-off from the heating wall without sliding, and the criterion for bubble lift-off from the heating wall is defined according to the condition $\sum F_y = 0$, at which point, the bubble will lift-off from the heating wall.

4.2. Analysis of mechanism of bubble departure

In order to predict the bubble departure diameter by analysis of force acting on the bubble, the interface parameters of a typical bubble, such as bubble contact diameter, d_w, bubble

inclination angle, θ, upstream and downstream contact angle, α and β, must be measured. Based on the experimental observation of bubble behavior by Xu et al. [14], d_w, θ, α and β can be set as $0.45d_b$, 45°,40°, and 10°, respectively. The bubble departure diameters under different thermal hydraulic conditions are predicted by solving the balance model of forces. The predictions of the bubble departure diameter are compared by 48 experimental data in both vertical and inclined conditions. **Figure 11** shows the predicted result agrees with experimental data.

The forces acting on the bubble in the x direction and y direction are calculated by using the balance model of forces in order to analyze the mechanism of bubble departing from the nucleation sites. **Table 1** shows the value of different forces acting on the bubble just departing from the nucleation sites.

The prediction of results indicates that a bubble will slide along the heating wall before lift-off because the condition $\sum F_x = 0$ is violated prior to the condition $\sum F_y = 0$, which is accorded with the visual experimental observation. As is seen from **Table 1**, the bubble growth force is much less than that of other forces due to the lower growth rate of the bubble, and it is negligible in the current case. The buoyancy force, quasi-steady drag force, and surface tension force are the main forces controlling the bubble departure.

4.3. Analysis of mechanism of sliding bubble motion

According to the experimental results, the inclination angle of the bubble approached 0 during the bubble sliding along the heating wall, and so the x components of the growth and surface tension forces are approximately 0. The balance of forces acting on a single bubble at the x direction is expressed as

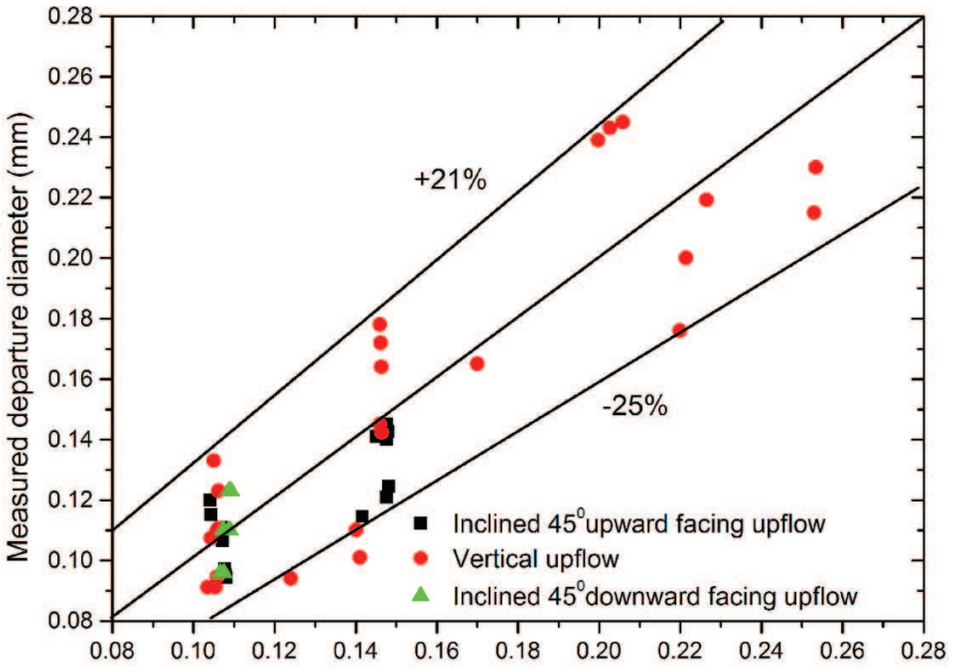

Figure 11. Comparison between predicted and measured results [14].

F_{bx}	F_{qs}	F_{sx}	F_{amx}	ΣF_x	F_{by}	F_{sy}	F_{amy}	F_{sl}	F_h	F_{cp}	ΣF_y
1.4E-08	6.1E-08	-7.5E-08	-1.1E-12	8.0E-11	1.1E-09	-8.5E-06	-9.9E-14	3.1E-08	3.2E-08	1.2E-06	-7.3E-06
1.4E-08	6.3E-08	-7.7E-08	-1.1E-12	1.3E-12	4.6E-09	-8.8E-06	-9.7E-14	3.2E-08	3.5E-08	1.2E-06	-7.5E-06
1.6E-08	7.3E-08	-8.9E-08	-5.6E-13	1.8E-10	4.5E-09	-1.0E-05	-4.9E-14	3.8E-08	5.2E-08	1.6E-06	-8.4E-06
2.0E-09	7.9E-08	-8.1E-08	-2.2E-12	2.1E-10	-2.6E-10	-4.6E-06	-2.0E-13	9.1E-08	6.1E-08	6.5E-07	-3.8E-06

Table 1. The force acting on the typical bubble (unit: N).

$$(\rho_l - \rho_v)V_b g \sin\Phi + \frac{1}{2}C_D\rho_l\pi a^2(u - v_x)|u - v_x| - \frac{1}{2}\cdot\frac{4}{3}\pi\rho_l a^3\frac{dv_x}{dt} + 2\pi\rho_l a^2(U - v_x)\dot{a} = m_b\frac{dv_x}{dt} \quad (27)$$

In order to solve the above differential equation, the initial condition is defined as $v(t_{\text{depart}}) = 0$, i.e., v is 0 when the vapor bubble just departs from the nucleation site and t_{depart} is the departure time of the vapor bubble. In our previous work [31], the sliding bubble velocities for pool and flow boiling in an ordinary size channel were obtained and the predicted results agreed with the experimental data of Maity [32]. However, the above balance of force is (27) was directly used to calculate the sliding bubble velocity in a narrow rectangular channel, it is found that the predicted result is not reasonable, and the force acting on the bubble is need to re-analyzed. The added-mass force is associated with the bubble growth rate and rate of change of bubble velocity. Some researchers showed that flow and heat transfer in a narrow rectangular channel were different with that in an ordinary size channel. In this experiment, the results show that the bubble grows slowly in a narrow rectangular channel and the bubble departure time is longer. This indicates that the size of a narrow channel inhibits bubble growth and departure. While the added-mass force were developed in an ordinary size channel by Thorncroft et al. [23]. Based on 72 experimental data on the sliding bubble velocity in a narrow rectangular channel, the value of the empirical constant C used for the evaluation of added-mass force is proposed, and the added-mass forces is expressed as:

$$F_{am} = C\left[\frac{1}{2}\cdot\frac{4}{3}\pi\rho_l a^3\left(\frac{dU}{dt} - \frac{dv_x}{dt}\right) + 2\pi\rho_l a^2(U - v_x)\dot{a}\right] \quad (28)$$

When the empirical constant C is 13.4, the prediction results agree with the experimental results.

Figure 12 shows the sliding bubble velocity against time for vertical flow boiling under the conditions of a bulk velocity of 0.143 m/s. As is seen from **Figure 12**, the predicted trends of the sliding bubble velocity agree with the experimental data. The sliding bubble velocity increases with increasing time, but the trend of an increase in the sliding bubble velocity decreases gradually as time increases. At about 14 ms, the sliding bubble velocity is higher than the local liquid velocity of the center of mass of the bubble. At about 50 ms, the sliding bubble velocity is almost equal to the bulk velocity. **Figure 13** shows the forces acting on the sliding bubble against time. The buoyancy gradually increases with increasing time, but the trend of an increase in the buoyancy is small, this is because the bubble growth rate is low. The buoyancy is the driving force to promote the bubble to slide along the surface in vertical flow boiling. At initial moment, the quasi-steady drag force is the driving force to promote the bubble to slide along the surface. At about 14 ms, the sliding bubble velocity exceeds the local liquid velocity

http://dx.doi.org/10.5772/intechopen.74608

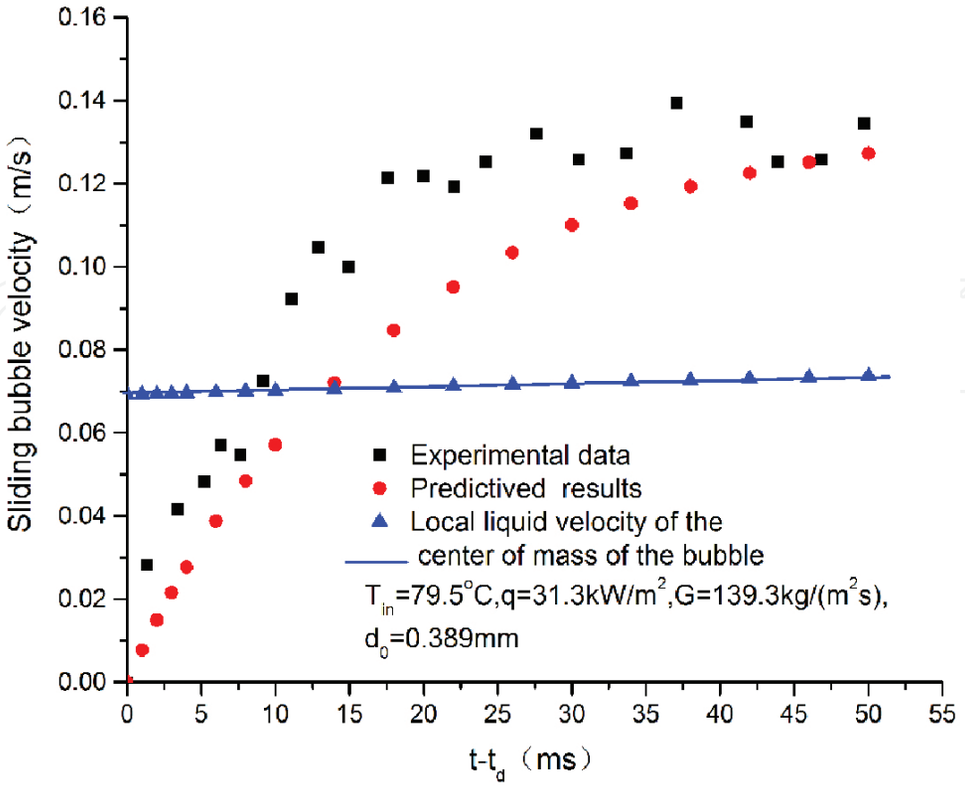

Figure 12. Sliding bubble velocity for vertical flow.

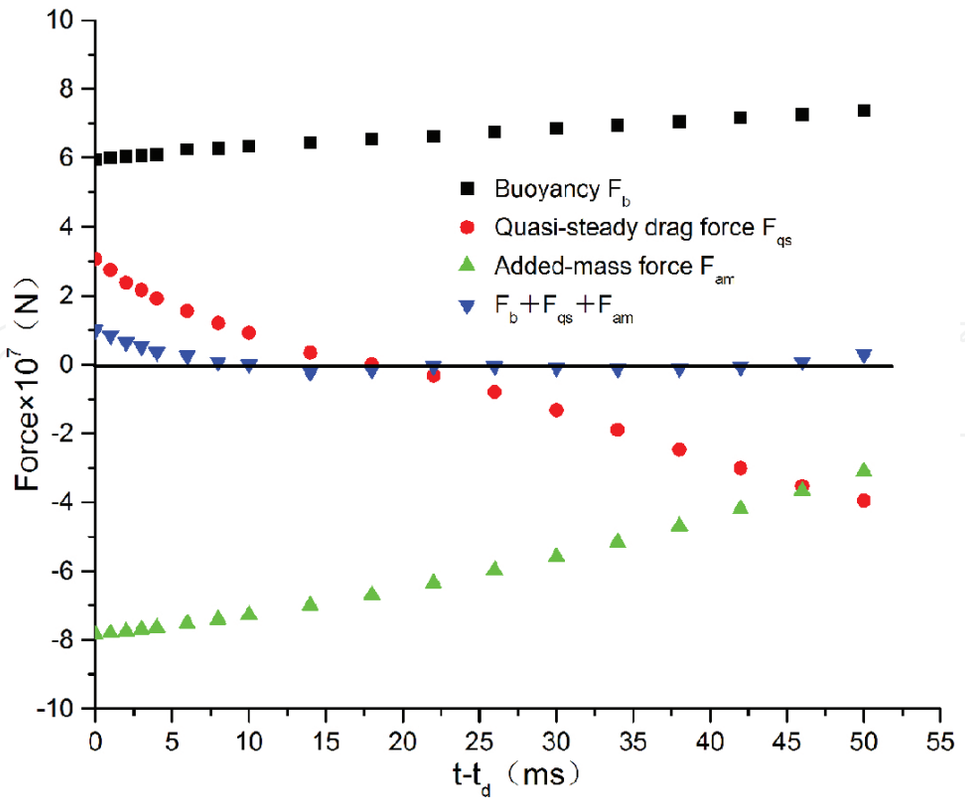

Figure 13. Forces acting on the sliding bubble for vertical flow.

and therefore, the quasi-steady drag force will become the resistance, which prevents the bubble from sliding along the surface. The quasi-steady drag force gradually increases because of an increasing difference between the sliding bubble velocity and the liquid velocity. During this process of the bubble sliding motion, the added-mass force is always a resistance to prevent the bubble from sliding along the surface. As the time increases, since the sliding bubble velocity exceeds the local liquid velocity, and therefore the shear lift force in the y direction will push the bubble against the wall, maybe this is cause of the bubble sliding along the surface in a vertical channel.

Figure 14 shows the sliding bubble velocity against time for in inclined 45° upward facing upflow boiling under the conditions of a bulk velocity of 0.143 m/s. As is seen from **Figure 14**, the predicted trends of the sliding bubble velocity agree with the experimental data. The trends of the sliding bubble velocity against time are similar to the above in **Figure 14**. The sliding bubble velocity increases quickly at the initial moment, but the trend of an increase in the sliding bubble velocity decreases gradually as the time increases. The buoyancy in the x direction is the driving force to promote the bubble to slide along the surface, as shown in **Figure 15**. At about 5 ms, the sliding bubble velocity is higher than the local liquid velocity of the center of mass of the bubble, and therefore the quasi-steady drag force will become the resistance, which prevents the bubble from sliding along the surface. At initial moment, the added-mass force is a resistance to prevent the bubble from sliding along the surface. At about 9 ms, the added-mass force will become a driving force to promote the bubble to slide along the surface. As the time increases, since the sliding bubble velocity exceeds the local liquid

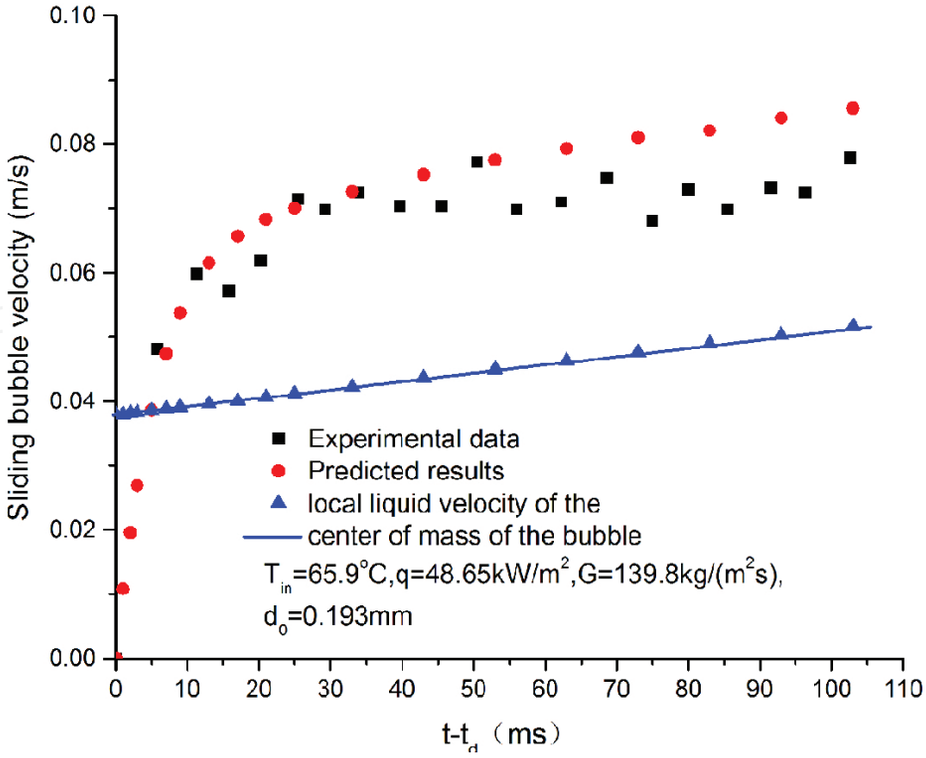

Figure 14. Sliding bubble velocity in inclined 45° upward facing upflow.

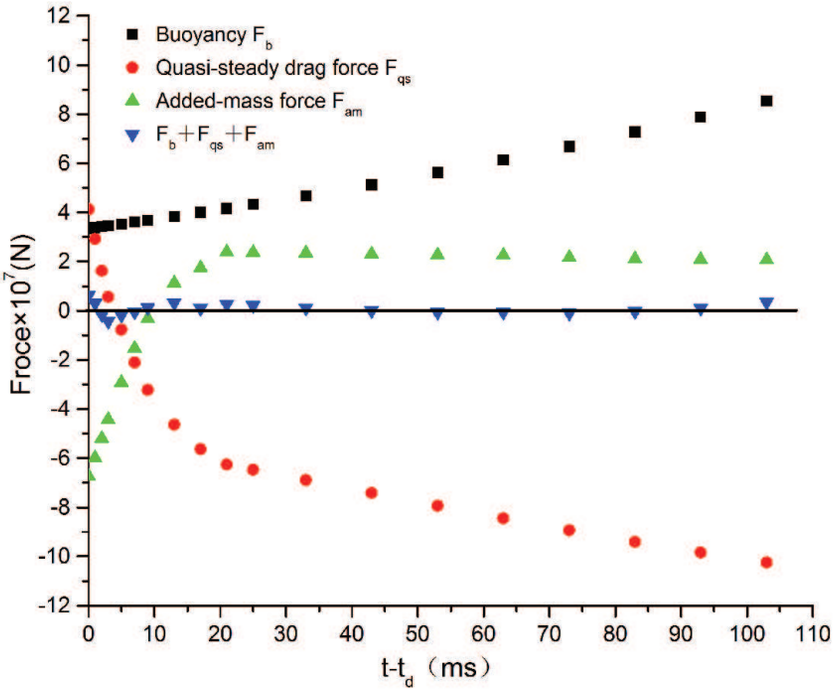

Figure 15. Force acting on the sliding bubble in inclined 45° upward facing upflow.

velocity of the center of mass of the bubble, and therefore the shear lift force in the y direction will push the bubble against the wall. The buoyancy in the y direction promotes the bubble lift-off from the surface.

5. Conclusions

Experimental and theoretical studies on bubble dynamics in a narrow rectangular channel are proposed in this chapter. A high speed digital camera is applied to capture bubble behaviors from the narrow side and wide side of the narrow rectangular channel. Bubble growth rate, bubble departure diameter, bubble interface parameter and others were obtained according to the observation. The bubbles always slide along the heating wall after departing from the nucleation sites. During the process of the sliding bubble motion along the heating wall, the upstream and downstream contact angle is almost equal. The phenomenon on bubble lift-off from the heating wall is not observed in vertical flow boiling with low heat flux in the isolated bubble region. The bubble tends to lift-off from the heating wall after sliding some distance in inclined upward facing upflow boiling and in vertical downflow boiling.

An analysis of force balance on a growing bubble is performed to analyze the mechanism of bubble departure, slide and lift-off behavior in the narrow channel. The bubble growth force is much less than the other forces acting on a bubble, and the buoyancy force, surface tension force, and quasi-steady drag force are the main forces controlling the bubble departure. The buoyancy, quasi-steady drag force, and added-mass force in the flow direction are the main

forces controlling the sliding bubble motion along the heating wall. As the time increases, since the sliding bubble velocity exceeds the local liquid velocity of the center of mass of the bubble, and therefore the shear lift force in the y direction will push the bubble against the wall.

Acknowledgements

This work is supported by the National Natural Science Foundation of China (No.11475161 and 51106142).

Nomenclature

F_x	composition of forces in the x direction
F_y	composition of forces in the y direction
F_{qs}	quasi-steady drag force
F_b	buoyancy
F_{sl}	shear lift force
F_s	surface tension force
F_{am}	added-mass force
F_{cp}	contact pressure force
F_h	hydrodynamic pressure force
V_b	bubble volume
q	heat flux
G	mass flux
u	local liquid velocity of the center of mass of the bubble
v	bubble velocity
t	time
T	temperature
d_w	bubble contact diameter
τ_w	wall shear stress
g	gravitational acceleration
r	bubble radius

$a(t)$	bubble growth rate
Re_b	bubble Reynolds number
U	bulk velocity,
C_f	friction coefficients
λ	friction factor
D_h	hydraulic equivalent diameter
R	ratio of the bubble contact diameter to bubble departure diameter
C	empirical constant

Greek symbols

a	upstream contact angle
β	downstream contact angle
θ	inclination angle
ρ_l	density of liquid,
ρ_v	density of bubble
γ	liquid kinematic viscosity
Φ	incline angle of the heating wall

Subscripts

x	direction parallel to the heating wall
y	direction normal to the heating wall
b_x	direction parallel to bulk flow
b_y	direction normal to the heating wall
b_z	direction perpendicular to flow
in	inlet

Author details

Xu Jianjun*, Xie Tianzhou, Chen Bingde and Bao Wei

*Address all correspondence to: xujjun2000@sohu.com

CNNC Key Laboratory on Nuclear Reactor Thermal Hydraulics Technology, Nuclear Power Institute of China, Chengdu, China

References

[1] Peng XF, Wang BX. Forced-convection and flow boiling heat transfer for liquid flow through micro-channels. International Journal of Heat and Mass Transfer. 1993;**36**(14): 3421-3427. DOI: 10.1016/0017-9310(93)90160-8

[2] Mishimal K, Mibiki T, Nishihara H. Some characterstics of gas-liguid flow in narrow rectangular duct. International Journal of Multiphase Flow. 1993;**19**(1):l15-124. DOI: 10.1016/0301-9322(93)90027-R

[3] Tran TN, Wambsganss MW, France DM. Small circular- and rectangular-channel boiling with two refrigerants. International Journal of Multiphase Flow. 1996;**22**(3):485-498. DOI: 10.1016/0301-9322(96)00002-X

[4] Jiang L, Wong M, Zohar Y. Forced convection boiling in a micro-channel heat sink. Journal of Microelectromechanical Systems. 2001;**10**:80-87. DOI: 10.1109/84.911095

[5] Kandikar SG. Fundamental issues related to flow boiling in minichannels and microchannels. Experimental Thermal and Fluid Science. 2002;**26**(2–4):389-407. DOI: 10.1016/S0894-1777(02) 00150-4

[6] Piasecka M, Hozejowska S, Poniewski ME. Experimental evaluation of flow boiling incipience of subcooled fluid in a narrow channel. International Journal of Heat and Fluid Flow. 2004;**25**(2):159-172. DOI: 10.1016/j.ijheatfluidflow.2003.11.017

[7] Lie YM, Lin TF. Saturated flow boiling heat transfer and associated bubble characteristics of R-134a in a narrow annular duct. International Journal of Heat and Mass Transfer. 2005;**48**(25–26):5602-5615. DOI: 10.1016/j.ijheatmasstransfer.2005.05.013

[8] Lie YM, Lin TF. Subcooled flow boiling heat transfer and associated bubble characteristics of R-134a in a narrow annular duct. International Journal of Heat and Mass Transfer. 2006;**49**(13–14):2077-2089. DOI: 10.1016/j.ijheatmasstransfer.2005.11.032

[9] Cheng P, Wang GD, Quan XJ. Recent work on boiling and condensation in microchannels. Journal of Heat Transfer. 2009;**131**(4):1-15. DOI: 10.1115/1.3072906

[10] Yu W, France DM, Wambsganss MW, Hull JR. Two-phase pressure drop, boiling heat transfer, and critical heat flux to water in a small-diameter horizontal tube. International Journal of Multiphase Flow. 2002;**28**(6):927-941. DOI: 10.1016/S0301-9322(02)00019-8

[11] Chen DQ, Pan LM, Yuan DW, Wang XJ. Dual model of bubble growth in vertical rectangular narrow channel. International Communications in Heat and Mass Transfer. 2010; **37**(8):1004-1007. DOI: 10.1016/j.icheatmasstransfer.2010.06.023

[12] Chen DQ, Pan LM, Ren S. Prediction of bubble detachment diameter in flow boiling based on force analysis. Nuclear Engineering and Design. 2012;**243**:263-271. DOI: 10.1016/j.nucengdes.2011.11.022

[13] Xu JJ, He JS, Chen BD, Huang YP, Yan X, Yuan DW. Experimental visualization of sliding bubble dynamics in a vertical narrow rectangular channel. Nuclear Engineering and Design. 2013;**261**(8):156-164. DOI: 10.1016/j.nucengdes.2013.02.055

[14] Xu JJ, Chen BD, Xie TZ. Experimental and theoretical analysis of bubble departure behavior in narrow rectangular channel. Progress in Nuclear Energy. 2014;**77**(4):1-10. DOI: 10.1016/j.pnucene.2014.06.002

[15] Xu JJ, He JS, Chen BD, Wang XJ. Visualization of behavior of subcooled boiling bubbles in narrow rectangular slits. Journal of Power Engineering. 2007;**27**(3):389-392. DOI: 10.3321/j.issn:1000-6761.2007.03.020

[16] Cornwell K. The influence of bubbly flow on boiling from a tube in a bundle. International Journal of Heat and Mass Transfer. 1990;**33**(23):2579-2584. DOI: 10.1016/0017-9310(90)90193-X

[17] Thorncroft GE, Klausner JF, Mei R. An experimental investigation of bubble growth and detachment in vertical upflow and downflow boiling. International Journal of Heat and Mass Transfer. 1998;**41**:3857-3871. DOI: 10.1016/S0017-9310(98)00092-1

[18] Thorncroft GE, Klausner JF. The influence of vapor bubble sliding on forced convection boiling heat transfer. Journal of Heat Transfer. 1999;**121**(1):73-79. DOI: 10.1115/1.2825969

[19] Kenning DBR, Bustnes OE, Yan Y. Heat transfer to a sliding vapour bubble. Multiphase Science Technology. 2000;**14**(1):75-94. DOI: 10.1615/MultScienTechn.v14.i1.20

[20] Li X, Hollingsworth K, Witte LC. Vapor bubble rise under a heated inclined plate. Experimental Thermal and Fluid Science. 2007;**32**(2):529-544. DOI: 10.1016/j.expthermflusci.2007.06.003

[21] Levy S. Forced convection subcooled boiling–prediction of vapor volumetric fraction. International Journal of Heat and Mass Transfer. 1967;**10**(7):951-965. DOI: 10.1016/0017-9310(67)90071-3

[22] Klausner JF, Mei R, Bernhard DM, Zeng LZ. Vapor bubble departure in forced convection boiling. International Journal of Heat and Mass Transfer. 1993;**36**(6):651-662. DOI: 10.1016/0017-9310(93)80041-R

[23] Thorncroft GE, Klausner JF, Mei R. Bubble force and detachment models. Multiphase Science and Technology. 2001;**13**(3&4):35-76. DOI: 10.1615/MultScienTechn.v13.i3-4.20

[24] Situ R, Hibiki T, Ishii M, Mori M. Bubble lift-off size in forced convective subcooled boiling flow. International Journal of Heat and Mass Transfer. 2005;**48**(24–25):5536-5548. DOI: 10.1016/j.ijheatmasstransfer.2005.06.031

[25] Cho Yun J, Yum SB, Lee JH, Park GC. Development of bubble departure and lift-off diameter models in low heat flux and low flow velocity conditions. International Journal of Heat and Mass Transfer. 2011;**54**(15–16):3234-3244. DOI: 10.1016/j.ijheatmasstransfer.2011.04.007

[26] Zuber N. The dynamics of vapor bubbles in nonuniform temperature fields. International Journal of Heat and Mass Transfer. 1961;**2**(1):83-98. DOI: 10.1016/0017-9310(61)90016-3

[27] Zeng LZ, Klausner JF, Mei R. A unified model for the prediction of bubble detachment diameters in boiling systems—II. Flow boiling. International Journal of Heat and Mass Transfer. 1993;**36**(9):2271-2279. DOI: 10.1016/S0017-9310(05)80112-7

[28] Delnoij E, Kuipers JAM, van Swaaij WPM. Dynamic simulation of gas–liquid two-phase flow: Effect of column aspect ratio on the flow structure. Chemical Engineering Science. 1997;**52**(21–22):3759-3772. DOI: 10.1016/S0009-2509(97)00222-4

[29] Saffman PG. The lift on a small sphere in a slow shear flow. Journal of Fluid Mechanics. 1965;**22**(2):385-400. DOI: 10.1017/S0022112065000824

[30] Mei R, Klausner JF. Shear lift force on spherical bubbles. International Journal of Heat and Fluid Flow. 1994;**15**(1):62-65. DOI: 10.1016/0142-727X(94)90031-0

[31] Xu JJ, Chen BD, Wang XJ. Prediction of sliding bubble velocity and mechanism of sliding bubble motion along the surface. Journal of Enhanced Heat Transfer. 2010;**17**(2):111-124. DOI: 10.1615/JEnhHeatTransf.v17.i2.10

[32] Maity S. Effect of velocity and gravity on bubble dynamics [thesis]. University of California. 2000